Acta Mech 195, 263–274 (2008)
DOI 10.1007/s00707-007-0546-5
Printed in The Netherlands

Acta Mechanica

Dedicated to Professor Franz Ziegler on the occasion of his 70th birthday

Steady-state creep of a pressurized thick cylinder in both the linear and the power law ranges

H. Altenbach, Y. Gorash, K. Naumenko

Center of Engineering Sciences, Martin-Luther-University Halle-Wittenberg, Halle, Germany

Received 9 October 2007; Accepted 21 November 2007; Published online 15 January 2008

Summary. The classical solution of the steady-state creep problem for a pressurized thick-walled cylinder is based on the power law constitutive equation. Several heat resistant steels show, however, the linear dependence of the creep rate on the applied stress within a certain stress range. In this paper we apply an extended constitutive equation which includes both the linear and the power law stress dependencies. The material constants are identified for the 9Cr1MoVNb steel at 600 °C. We recall the boundary value problem of steady-state creep for the thick cylinder under the plane strain condition. We present an approximate solution illustrating the stress redistributions as a result of the creep process. The analysis shows that for the certain range of the internal pressure both the linear and the power law creep must be taken into account. In this case the results according to the extended constitutive model essentially differ from the classical ones. The obtained solution is also applied to verify the developed user-defined creep material subroutine inside a commercial finite element code.

1 Introduction

Many components of power generation equipment are subjected to high temperature environment and complex loading conditions over a long time. Design procedures and residual life assessments for pipe systems, rotors, turbine blades, turbine and valve casings, etc., require the accounting for creep and damage processes. The aim of "creep modeling for structural analysis" is the development of methods to predict time-dependent changes of stress and strain states in engineering structures up to the critical stage of creep rupture, see, e.g., [1], [2]. Structural analysis under creep conditions requires a reliable constitutive model which reflects time-dependent creep deformations and processes accompanying creep like hardening/recovery and damage. An important feature of the creep constitutive equation is the response function of the applied stress which should extrapolate the creep data usually obtained under increased stress in the laboratory to the in-service loading conditions. A typical example is the power law which often finds application because of smaller effort in identification of material constants and simplicity in structural analysis. However, it is known from the materials science that the "power law creep mechanism" operates only for a specific

Correspondence: Holm Altenbach, Center of Engineering Sciences, Martin-Luther-University Halle-Wittenberg, 06099 Halle, Germany
e-mail: holm.altenbach@iw.uni-halle.de

stress range and may change to the linear, e.g. diffusion type mechanism for the low stress values [3]. Furthermore, as shown in the recently published experimental data [4], [5], advanced heat resistant steels may exhibit the transition from the linear to the power law creep at the stress levels, relevant for engineering applications.

In this paper we address the creep analysis of heat resistant steels and thick-walled structural components for a wide stress range including low and moderate stress values. Based on the available experimental data the creep constitutive equation which describes both the linear and the power law creep is discussed. As an example for the structural mechanics application we recall the classical problem of a pressurized thick cylinder under plane strain conditions. This problem is widely discussed in textbooks on creep mechanics, e.g., [1], [6], [7], and usually applied as a benchmark problem to verify the finite element solutions, e.g., [8]. However, the available results are only valid for either the linear or the power law creep ranges. We present an extended solution by including the transition from the linear to the power law creep. Based on the results we discuss the validity range of the classical approach.

2 Constitutive model

Within the phenomenological approach to the creep modeling one usually starts with the constitutive equation for the minimum (secondary) creep rate. To characterize the hardening/recovery and damage processes this equation is generalized by introduction of internal state variables and appropriate evolution equations. The conventional constitutive equations characterize the secondary creep rate by the power law stress function and include the effect of tertiary creep by means of the scalar valued damage parameter. An example is the following model [9]:

$$\dot{\boldsymbol{\varepsilon}}^{\mathrm{cr}} = \frac{3}{2} a \Big(\frac{\sigma_{\mathrm{vM}}}{1-\omega} \Big)^{n} \frac{\boldsymbol{s}}{\sigma_{\mathrm{vM}}}, \quad \dot{\omega} = b \frac{[\alpha \sigma_{\mathrm{T}} + (1-\alpha)\sigma_{\mathrm{vM}}]^{k}}{(1-\omega)^{l}} \tag{1}$$

with

$$\sigma_{\mathrm{vM}} = \sqrt{\frac{3}{2} \boldsymbol{s} \cdot \cdot \boldsymbol{s}}, \quad \sigma_{\mathrm{T}} = \frac{1}{2}(\sigma_I + |\sigma_I|).$$

In this notation $\dot{\boldsymbol{\varepsilon}}^{\mathrm{cr}}$ is the creep rate tensor, $\boldsymbol{\sigma}$ is the stress tensor, $\boldsymbol{s}$ is the stress deviator, σ_{vM} is the von Mises equivalent stress, σ_{T} is the maximum tensile stress, σ_I is the first principal stress, and ω is the damage parameter. The weighting factor α characterizes the influence of the principal damage mechanisms (σ_{T}-controlled or σ_{vM}-controlled). a, b, n, k and l are material constants.

To identify the material constants in Eqs. (1), experimental data of uni-axial creep up to rupture are required. The identification procedure is presented for example in [10]. The model (1) has been widely used to characterize creep and long-term strength of materials and structures. Examples of material constants as well as structural mechanics applications can be found in [2], [10]–[13] among others. However, the model (1) guarantees the correct prediction of the creep and the damage rates only for a certain stress range. To discuss the range of validity let us consider the uni-axial stress state with the tensile stress σ. In this case Eqs. (1) provide the following relations

$$\dot{\varepsilon}^{\mathrm{cr}}_{\mathrm{min}} = a\sigma^{n}, \quad t_* = \frac{1}{A\sigma^{k}}, \quad \varepsilon^{\mathrm{cr}}_{*} = B\sigma^{n-k}, \quad A \equiv (l+1)b, \quad B \equiv \frac{a}{b(l+1-n)}, \tag{2}$$

where $\dot{\varepsilon}^{\mathrm{cr}}_{\mathrm{min}}$ is the minimum creep rate, t_* is the time to fracture and $\varepsilon^{\mathrm{cr}}_{*}$ is the creep strain before fracture (creep ductility). The plots of Eqs. (2) in a double logarithmic scale represent straight lines. Figure 1a shows a typical dependence of the minimum creep rate on the applied stress for advanced

heat-resistant steels. Within the range $0 \le \sigma \le \sigma_0$, where σ_0 is the transition stress, the creep rate is a nearly linear function of the stress. The "moderate" stress range is characterized by the power law creep. The creep exponent takes usually the values between 3 and 12 depending on the material, type of alloying and processing conditions. Within the region of "high" stresses the power law breakdown is usually observed. Figure 1b illustrates a typical long-term strength curve, i.e. the dependence of time to creep fracture on the applied stress. The available data for the range of "low" stresses suggest that the dominant damage mechanism is the nucleation and growth of intergranular cavities and microcracks [14]. For moderate stresses the damage evolution is determined by the mixed (brittle–ductile) mode. The additional damage mechanisms are the microstructure degradation processes, e.g. the subgrain coarsening and coarsening of carbide precipitates [15]. For "high" stress values the fracture mode is primarily ductile and the uni-axial specimen necks down as a result of excessive deformation.

Here let us focus on the analysis of steady-state creep. Processes associated with the microstructural degradation will be ignored. Although such an approach does not allow to predict the time to creep fracture, it provides a first estimation of the stress redistribution in a structure. Figure 2 shows the experimental data for 9Cr1MoVNb steel at 600 °C after [4], [5]. In the "low" stress range the creep rate can be well approximated by a linear function of the applied stress. For the "moderate" stress range the considered steel exhibits power law creep with the creep exponent $n = 12$. To describe the creep behavior for both the linear and power law creep ranges various functions of stress, which are more or less physically motivated, have been proposed. Overviews are presented in [7] and [16] among others. One example is the hyperbolic sine law $\dot{\varepsilon} = A \sinh(B\sigma)$, applied in [17]–[19] to characterize minimum creep rate of various materials. However, for the considered steel this equation describes well only the linear creep range, Fig. 2. In what follows let us assume the minimum creep rate to be the sum of the linear and the power law stress functions

$$\dot{\varepsilon} = a\frac{\sigma}{\sigma_0} + a\left(\frac{\sigma}{\sigma_0}\right)^n = a\frac{\sigma}{\sigma_0}\left[1 + \left(\frac{\sigma}{\sigma_0}\right)^{n-1}\right], \tag{3}$$

where σ_0 is the "transition stress". With $n = 12$ and $\sigma_0 = 100$ MPa the model (3) provides a good description of the minimum creep rate for both the linear and the power law creep ranges, Fig. 2.

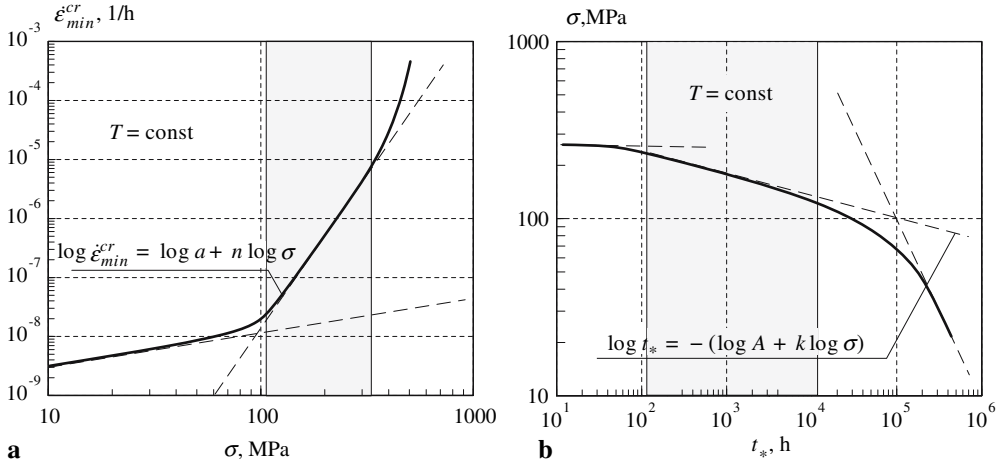

Fig. 1. Sketch of creep behavior for heat resistant steels. **a** Minimum creep rate versus stress, **b** stress versus time to fracture

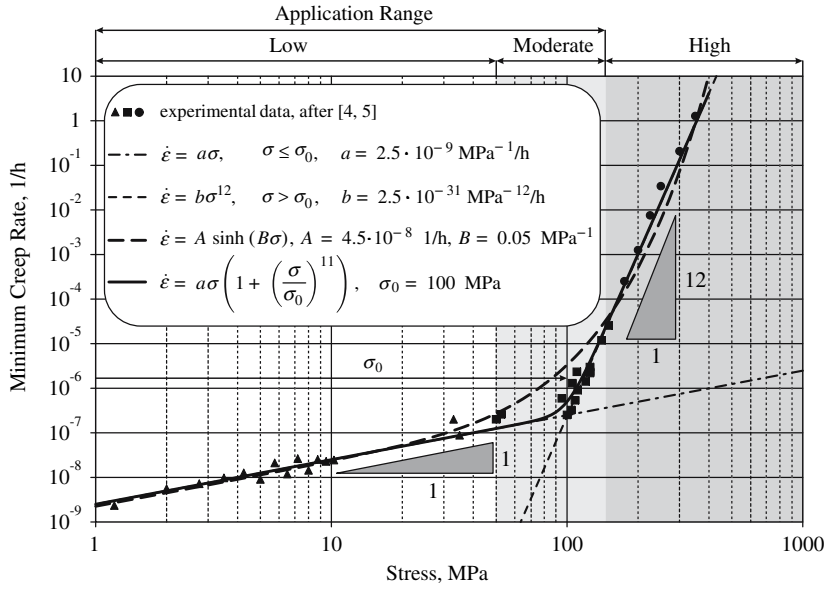

Fig. 2. Minimum creep rate versus stress for 9Cr1MoVNb steel at 600 °C

Many examples of structural analysis, e.g., [2], show, that the ranges of "low" and "moderate" stresses are mostly important for engineering applications. Therefore, for structures made from advanced heat resistant steels the use of the power law stress function may lead to a significant underestimation of the creep rate for the "low" stress values.

Equation (3) can only be applied to the case of constant temperature. For non-isothermal conditions the material constants a and σ_0 should be replaced by functions of temperature. The experimental data presented in [4] for different temperatures suggest that with an increase of the temperature the transition stress σ_0 decreases, while the constant a increases. In what follows let us assume isothermal conditions for the sake of brevity.

The structural analysis requires a constitutive model of creep under multi-axial stress states. Following the creep theory proposed by Odqvist [20] the creep rate tensor $\dot{\boldsymbol{\varepsilon}}^{\mathrm{cr}}$ is defined by the creep potential W and the flow rule

$$\dot{\boldsymbol{\varepsilon}}^{\mathrm{cr}} = \frac{\partial W}{\partial \boldsymbol{\sigma}}, \quad W = W(\boldsymbol{\sigma}, T). \tag{4}$$

For isotropic materials the creep potential must satisfy the restriction

$$W\left(\boldsymbol{Q} \cdot \boldsymbol{\sigma} \cdot \boldsymbol{Q}^T\right) = W(\boldsymbol{\sigma}) \tag{5}$$

for any symmetry transformation $\boldsymbol{Q}$, $\boldsymbol{Q} \cdot \boldsymbol{Q}^T = \boldsymbol{I}$, $\det \boldsymbol{Q} = \pm 1$. From this follows that the potential depends only on the three invariants of the stress tensor. With the principal invariants

$$J_1(\boldsymbol{\sigma}) = \operatorname{tr} \boldsymbol{\sigma}, \quad J_2(\boldsymbol{\sigma}) = \frac{1}{2}[(\operatorname{tr} \boldsymbol{\sigma})^2 - \operatorname{tr} \boldsymbol{\sigma}^2], \quad J_3(\boldsymbol{\sigma}) = \det \boldsymbol{\sigma} = \frac{1}{6}(\operatorname{tr} \boldsymbol{\sigma})^3 - \frac{1}{2} \operatorname{tr} \boldsymbol{\sigma} \operatorname{tr} \boldsymbol{\sigma}^2 + \frac{1}{3} \operatorname{tr} \boldsymbol{\sigma}^3 \tag{6}$$

one can write

$$W(\boldsymbol{\sigma}) = W(J_1, J_2, J_3).$$

Any symmetric second rank tensor can be uniquely decomposed into the spherical and the deviatoric part. For the stress tensor the decomposition has the form

$$\boldsymbol{\sigma} = \sigma_{\mathrm{m}}\boldsymbol{I} + \boldsymbol{s}, \quad \mathrm{tr}\,\boldsymbol{s} = 0 \;\Rightarrow\; \sigma_{\mathrm{m}} = \frac{1}{3}\mathrm{tr}\,\boldsymbol{\sigma}.$$

With the principal invariants of the stress deviator

$$J_{2D} = -\frac{1}{2}\mathrm{tr}\,\boldsymbol{s}^2 = -\frac{1}{2}\boldsymbol{s}\cdot\cdot\boldsymbol{s}, \quad J_{3D} = \frac{1}{3}\mathrm{tr}\,\boldsymbol{s}^3 = \frac{1}{3}(\boldsymbol{s}\cdot\boldsymbol{s})\cdot\cdot\boldsymbol{s}$$

the potential takes the form $W = W(J_1, J_{2D}, J_{3D})$. Applying the rule for the derivative of a scalar valued function with respect to a second rank tensor one can obtain

$$\dot{\boldsymbol{\varepsilon}}^{\mathrm{cr}} = \frac{\partial W}{\partial J_1}\boldsymbol{I} - \frac{\partial W}{\partial J_{2D}}\boldsymbol{s} + \frac{\partial W}{\partial J_{3D}}\left(\boldsymbol{s}^2 - \frac{1}{3}\mathrm{tr}\,\boldsymbol{s}^2\boldsymbol{I}\right). \tag{7}$$

In the classical creep theory it is assumed that the inelastic deformation does not produce a significant change in volume. The spherical part of the creep rate tensor is neglected, i.e., $\mathrm{tr}\,\dot{\boldsymbol{\varepsilon}}^{\mathrm{cr}} = 0$. Setting the trace of (7) to zero results in

$$\mathrm{tr}\,\dot{\boldsymbol{\varepsilon}}^{\mathrm{cr}} = 3\frac{\partial W}{\partial J_1} = 0 \;\Rightarrow\; W = W(J_{2D}, J_{3D}),$$

and the first term in the right-hand side of Eq. (7) can be neglected. From this follows that the creep behavior is not sensitive to the hydrostatic stress state $\boldsymbol{\sigma} = -p\boldsymbol{I}$, where $p > 0$ is the hydrostatic pressure. The last term in the right-hand side of Eq. (7) is nonlinear with respect to the stress deviator $\boldsymbol{s}$. Equations of this type are called tensorial nonlinear equations, e.g., [1], [21]. They allow to consider some non-classical stress state dependencies or second-order effects of the material behavior. Within the engineering creep mechanics such effects are usually ignored. The assumption that the potential is a function of the second invariant of the stress deviator only, i.e. $W = W(J_{2D})$, leads to the classical von Mises type theory. In applications it is convenient to introduce the equivalent stress to compare the creep behavior under different stress states including the uni-axial tension. With the von Mises equivalent stress

$$\sigma_{\mathrm{vM}} = \sqrt{-3J_{2D}}$$

and $W = W(\sigma_{\mathrm{vM}}(\boldsymbol{\sigma}))$ the flow rule (4) results in

$$\dot{\boldsymbol{\varepsilon}}^{\mathrm{cr}} = \frac{\partial W(\sigma_{\mathrm{vM}})}{\partial \sigma_{\mathrm{vM}}}\frac{\partial \sigma_{\mathrm{vM}}}{\partial \boldsymbol{\sigma}} = \frac{\partial W(\sigma_{\mathrm{vM}})}{\partial \sigma_{\mathrm{vM}}}\frac{3}{2}\frac{\boldsymbol{s}}{\sigma_{\mathrm{vM}}}. \tag{8}$$

The second invariant of $\dot{\boldsymbol{\varepsilon}}^{\mathrm{cr}}$ can be calculated as follows:

$$\dot{\boldsymbol{\varepsilon}}^{\mathrm{cr}}\cdot\cdot\dot{\boldsymbol{\varepsilon}}^{\mathrm{cr}} = \frac{3}{2}\left[\frac{\partial W(\sigma_{\mathrm{vM}})}{\partial \sigma_{\mathrm{vM}}}\right]^2.$$

Introducing the notation $\dot{\varepsilon}^2_{\mathrm{vM}} = \frac{2}{3}\dot{\boldsymbol{\varepsilon}}^{\mathrm{cr}}\cdot\cdot\dot{\boldsymbol{\varepsilon}}^{\mathrm{cr}}$ and taking into account that $P = \dot{\boldsymbol{\varepsilon}}^{\mathrm{cr}}\cdot\cdot\boldsymbol{\sigma} \geq 0$, where P is the dissipation power, one can write

$$\dot{\boldsymbol{\varepsilon}}^{\mathrm{cr}} = \frac{3}{2}\dot{\varepsilon}_{\mathrm{vM}}\frac{\boldsymbol{s}}{\sigma_{\mathrm{vM}}}, \quad \dot{\varepsilon}_{\mathrm{vM}} = \frac{\partial W(\sigma_{\mathrm{vM}})}{\partial \sigma_{\mathrm{vM}}}. \tag{9}$$

The Odqvist creep theory assumes the power law type creep potential

$$W(\sigma_{\mathrm{vM}}) = \frac{a}{n+1}\sigma^{n+1}_{\mathrm{vM}}.$$

According to experimental data for the considered steel let us apply the potential

$$W(\sigma_{\mathrm{vM}}) = \frac{a}{2}\left(\frac{\sigma_{\mathrm{vM}}}{\sigma_0}\right)^2 + \frac{a}{n+1}\left(\frac{\sigma_{\mathrm{vM}}}{\sigma_0}\right)^{n+1}.$$

In this case the creep constitutive equation (9) takes the form

$$\dot{\boldsymbol{\varepsilon}}^{\mathrm{cr}} = \frac{3}{2}\frac{\dot{\varepsilon}_0}{\sigma_0}\left[1 + \left(\frac{\sigma_{\mathrm{vM}}}{\sigma_0}\right)^{n-1}\right]\boldsymbol{s}, \quad \dot{\varepsilon}_0 \equiv a\sigma_0 \tag{10}$$

with the following material constants:

$$\dot{\varepsilon}_0 = 2.5 \times 10^{-7}\,1/\mathrm{h}, \quad \sigma_0 = 100\,\mathrm{MPa}, \quad n = 12.$$

3 Governing equations for steady-state creep of thick cylinder

Consider a thick cylinder section loaded by internal pressure, Fig. 3. Let $\boldsymbol{v}$ be the vector characterizing the velocity of the material point. Assuming the plane strain state we may write

$$\boldsymbol{v} = v_r(r)\boldsymbol{e}_r \;\Rightarrow\; \nabla\boldsymbol{v} = (\nabla\boldsymbol{v})^T = \frac{\partial v_r}{\partial r}\boldsymbol{e}_r \otimes \boldsymbol{e}_r + \frac{v_r}{r}\boldsymbol{e}_\varphi \otimes \boldsymbol{e}_\varphi. \tag{11}$$

The condition of the volume constancy yields

$$\nabla \cdot \boldsymbol{v} = \frac{\partial v_r}{\partial r} + \frac{v_r}{r} = 0 \Rightarrow v_r = \frac{C}{r}, \tag{12}$$

where C is an integration constant. In what follows we apply the geometrically linear theory. In this case the symmetric part of the velocity gradient is the strain rate tensor

$$\dot{\boldsymbol{\varepsilon}} = \frac{C}{r^2}(\boldsymbol{e}_\varphi \otimes \boldsymbol{e}_\varphi - \boldsymbol{e}_r \otimes \boldsymbol{e}_r), \tag{13}$$

and the latter can be additively decomposed into the elastic and the creep part. The rate of the stress deviator is related to the rate of the deviatoric part of the elastic strain

$$\dot{\boldsymbol{s}} = 2G(\dot{\boldsymbol{\varepsilon}} - \dot{\boldsymbol{\varepsilon}}^{\mathrm{cr}}), \tag{14}$$

where G is the shear modulus. If the hardening and the damage processes are negligible and the pressure is constant over time, then the steady state solution exists for which $\dot{\boldsymbol{s}} = \boldsymbol{0}$. With Eqs. (10), (13) and (14) we obtain

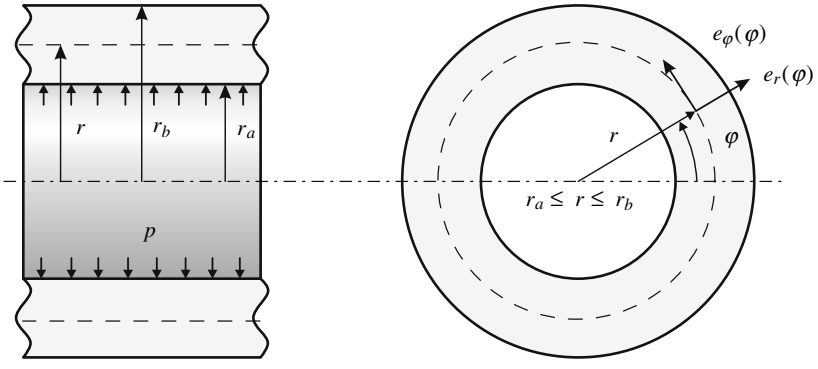

Fig. 3. Thick cylinder, geometry and loading

$$\frac{C}{r^2}(\boldsymbol{e}_\varphi \otimes \boldsymbol{e}_\varphi - \boldsymbol{e}_r \otimes \boldsymbol{e}_r) = \frac{3}{2}\frac{\dot{\varepsilon}_0}{\sigma_0}\left[1 + \left(\frac{\sigma_{\mathrm{vM}}}{\sigma_0}\right)^{n-1}\right]\boldsymbol{s}. \tag{15}$$

According to Eq. (15) the stress deviator and the von Mises equivalent stress have the following form:

$$\boldsymbol{s}(r) = s(r)(\boldsymbol{e}_\varphi \otimes \boldsymbol{e}_\varphi - \boldsymbol{e}_r \otimes \boldsymbol{e}_r) \;\Rightarrow\; \sigma_{\mathrm{vM}}(r) = \sqrt{3}s(r), \tag{16}$$

where the function $s(r)$ must be found from the following nonlinear equation

$$\frac{C}{r^2} = \frac{3}{2}\frac{\dot{\varepsilon}_0}{\sigma_0}\left[1 + \left(\frac{\sqrt{3}s(r)}{\sigma_0}\right)^{n-1}\right]s(r). \tag{17}$$

The classical approach to the steady state creep of the thick cylinder assumes the power law creep constitutive equation, e.g., [1], [6], [7]. In this case Eq. (17) simplifies to

$$\frac{C}{r^2} = \frac{3}{2}\frac{\dot{\varepsilon}_0}{\sigma_0}\left(\frac{\sqrt{3}s(r)}{\sigma_0}\right)^{n-1}s(r).$$

The mean stress σ_{m} must be found from the equilibrium condition

$$\nabla\sigma_{\mathrm{m}} + \nabla\cdot\boldsymbol{s} = 0 \;\Rightarrow\; \frac{d\sigma_{\mathrm{m}}}{dr} = \frac{ds}{dr} + \frac{2}{r}s. \tag{18}$$

The radial stress σ_{r}, the hoop stress σ_φ and the axial stress σ_z are defined as follows:

$$\sigma_{\mathrm{r}} = \boldsymbol{e}_r\cdot\boldsymbol{\sigma}\cdot\boldsymbol{e}_r = \sigma_{\mathrm{m}} - s, \quad \sigma_\varphi = \boldsymbol{e}_\varphi\cdot\boldsymbol{\sigma}\cdot\boldsymbol{e}_\varphi = \sigma_{\mathrm{m}} + s, \quad \sigma_z = \boldsymbol{e}_z\cdot\boldsymbol{\sigma}\cdot\boldsymbol{e}_z = \sigma_{\mathrm{m}}. \tag{19}$$

The radial stress must satisfy the following boundary conditions:

$$\sigma_r(r_a) = -p, \quad \sigma_{\mathrm{r}}(r_b) = 0. \tag{20}$$

4 Solutions

Let us rewrite Eq. (17) in the normalized form

$$f(\tilde{s}) = \tilde{s} + \tilde{s}^n = \frac{\tilde{C}}{\eta^2}, \quad \tilde{s} \equiv \frac{s}{\sigma_0}\sqrt{3} = \frac{\sigma_{\mathrm{vM}}}{\sigma_0}, \quad \tilde{C} \equiv \frac{C}{\sqrt{3}\dot{\varepsilon}_0 r_a^2}, \quad \eta = \frac{r}{r_a}. \tag{21}$$

Since $f(\tilde{s})$ is a monotonically increasing function, an inverse function exists such that

$$\tilde{s} = f^{-1}(\tilde{C}/\eta^2). \tag{22}$$

With the boundary condition $\sigma_{\mathrm{r}}(1) = -p$ and Eqs. (18)–(20) the following equation can be derived:

$$\int_1^{1/\zeta} \frac{2}{r} f^{-1}(\tilde{C}/\eta^2)d\eta = \frac{\sqrt{3}p}{\sigma_0}, \quad \zeta = \frac{r_a}{r_b}. \tag{23}$$

By solving Eq. (23) the integration constant $\tilde{C}$ can be obtained. From Eqs. (18), (19) and (20) the following equations for the stress distributions along the radial coordinate η can be derived:

$$\sigma_{\mathrm{r}}(\eta,\tilde{C})=\frac{2\sigma_0}{\sqrt{3}}\int\limits_{1/\zeta}^{\eta}\frac{1}{\eta}f^{-1}(\tilde{C}/\eta^2)d\eta,\quad \sigma_{\varphi}(\eta,\tilde{C})=\frac{2\sigma_0}{\sqrt{3}}\left[\int\limits_{1/\zeta}^{r}\frac{1}{\eta}f^{-1}(\tilde{C}/\eta^2)d\eta+f^{-1}(\tilde{C}/\eta^2)\right]. \tag{24}$$

The classical solution to the steady-state creep of the thick cylinder is based on the power law stress function, e.g., [6]. It follows from Eqs. (21)–(24) by assuming $\tilde{s}\gg 1$. In this case

$$f(\tilde{s})=\tilde{s}^n\ \Rightarrow\ f^{-1}(\tilde{C}/\eta^2)=\frac{\tilde{C}^{1/n}}{\eta^{2/n}}.$$

Equation (23) yields

$$\tilde{C}^{1/n}=\frac{\sqrt{3}p}{\sigma_0}\frac{1}{n(1-\zeta^{2/n})}.$$

The normalized von Mises equivalent stress can be obtained from Eq. (22) as

$$\tilde{s}=\frac{\sqrt{3}p}{\sigma_0}\frac{1}{n(1-\zeta^{2/n})\eta^{2/n}}. \tag{25}$$

Equations (24) provide the following stress distributions:

$$\sigma_{\mathrm{r}}=-\frac{p}{1-\zeta^{2/n}}\left(\eta^{2/n}-\zeta^{2/n}\right),\quad \sigma_{\varphi}=\frac{p}{1-\zeta^{2/n}}\left(\zeta^{2/n}-\frac{n-2}{n}\eta^{2/n}\right). \tag{26}$$

According to Eq. (25) the normalized von Mises stress takes the minimum value on the outer surface of the cylinder, i.e. for $\eta=1/\zeta$

$$\tilde{s}_{\min}=\frac{\sqrt{3}p}{\sigma_0}\frac{\zeta^{2/n}}{n(1-\zeta^{2/n})}.$$

The classical solution can only be applied for $\tilde{s}_{\min}\gg 1$. In this case the cylinder "operates" in the power law creep range. For the normalized pressure we obtain

$$\frac{p}{\sigma_0}\gg\frac{n}{\sqrt{3}}\frac{1-\zeta^{2/n}}{\zeta^{2/n}}.$$

As an example let us assume $\zeta=0.5$. For 9Cr1MoVNb steel at 600 °C with $\sigma_0=100$ MPa and $n=12$ we find that $p\gg 0.848\sigma_0=84.8$ MPa.

On the other hand, if we set $\tilde{s}\ll 1$, then the linear creep range, i.e. $f(\tilde{s})=\tilde{s}$, can be assumed. The corresponding stress distributions follow from Eqs. (25) and (26) by setting $n=1$. The normalized von Mises stress takes the maximum value at the inner radius $\eta=1$,

$$\tilde{s}_{\min}=\frac{\sqrt{3}p}{\sigma_0}\frac{1}{1-\zeta^2}\ll 1.$$

With $\zeta=0.5$ and $\sigma_0=100$ MPa we find that cylinder "behaves" in the linear creep range for $p\ll 43.3$ MPa. We observe that for the considered steel the classical approach can be applied either for very high or for very low pressures.

To match the results the transition from the linear to the power law creep must be taken into account. In this case the inverse function f^{-1} and consequently the stress distributions cannot be presented in the closed analytical form. To obtain an approximate solution of Eqs. (21)–(24) two numerical procedures including the numerical integration and finding the root of a nonlinear algebraic equation are required. For the calculations we applied the Mathcad package. The input

parameters are the ratio of the cylinder radii ζ, the normalized pressure $\tilde{p} = p/\sigma_0$ and the creep exponent n. Figure 4 shows the dependence of the integration constant $\tilde{C}$ on the normalized pressure $\tilde{p}$ in the double logarithmic scale for the case $\zeta = 0.5$. Similar to the minimum creep rate versus stress dependence, Fig. 2, the linear, the transition and the power law ranges are observable. Figure 5 illustrates the dependence of the hoop stress on the normalized pressure for different values of ζ. The validity ranges of the classical solution can be recognized. For both the low and the high pressures the results do not depend on $\tilde{p}$ and agree with the classical solution (26) for $n = 1$ and $n = 12$. We observe that if the power law stress function would be applied then the hoop stress would be underestimated on the inner surface and overestimated on the outer surface. The range of validity of the power law creep depends on ζ and extends with an increase of ζ (decrease of the wall thickness). Therefore for thin walled pipes loaded by a moderate pressure the power law creep is a reasonable approximation. Figure 6 illustrates the stress distributions along the radial coordinate for the case $\zeta = 0.5$. For $\tilde{p} = 0.2$ the results agree with the classical solution assuming the linear creep. Let us note that for $n = 1$ the stress distributions (26) coincide with the Lamé solution of the linear elasticity problem. For $\tilde{p} = 0.9$ the results correspond to the power law creep solution. In this case the hoop stress relaxes down on the inner surface and increases on the outer surface. For moderate pressures usually encountered in the praxis the result differs from the classical one. The hoop stress still relaxes down on the inner surface but its maximum shifts towards the core layer of the cylinder.

In recent years the finite element method has become the widely accepted tool for structural analysis. The advantage of the finite element method is the possibility to simulate creep processes in real engineering structures with complex geometries, various types of loading and boundary conditions. To apply a general purpose finite element code a user-defined material subroutine which includes the specific creep constitutive model should be developed. To assess that the subroutine is correctly coded and implemented, results of finite element computations must be compared with reference solutions of benchmark problems. Several benchmark problems based on the creep constitutive model (1) are presented in [2], [22].

We incorporated the creep constitutive equation (10) into the ABAQUS finite element code. The results obtained by the approximate solution of Eqs. (21)–(24) do not involve the finite element meshing and can be applied to verify the finite element procedures. Let us note that the steady state creep problem of the thick cylinder in the power law creep range is the standard benchmark [8]. The geometrical data and the finite element model are assumed as given in the benchmark manual [8]. In the calculations we set $r_a = 25.4$ mm, $r_b = 50.8$ mm. The pipe section has been meshed by ten

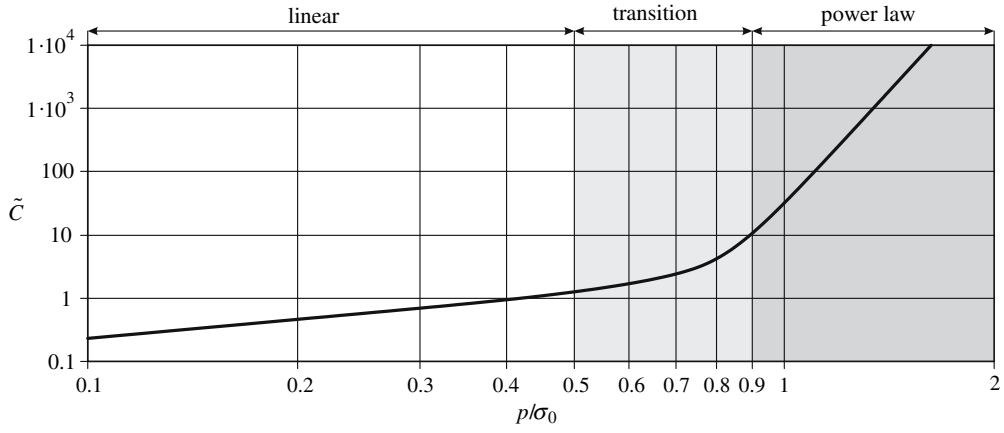

Fig. 4. Integration constant versus normalized pressure for $\zeta = 0.5$

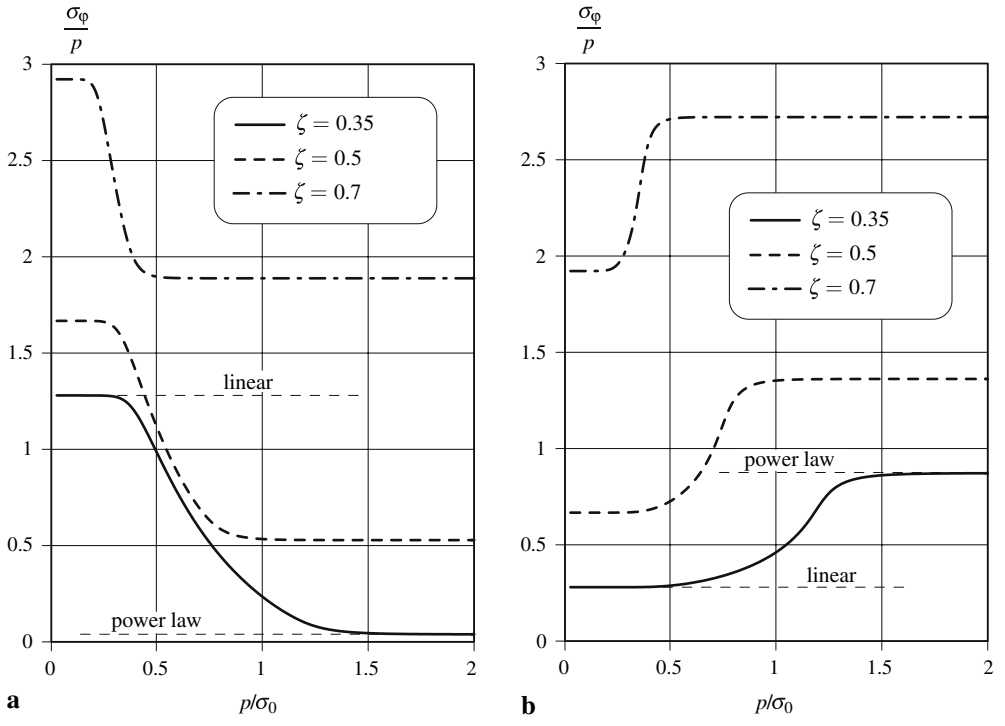

Fig. 5. Normalized hoop stress versus normalized pressure. **a** Inner surface, **b** outer surface

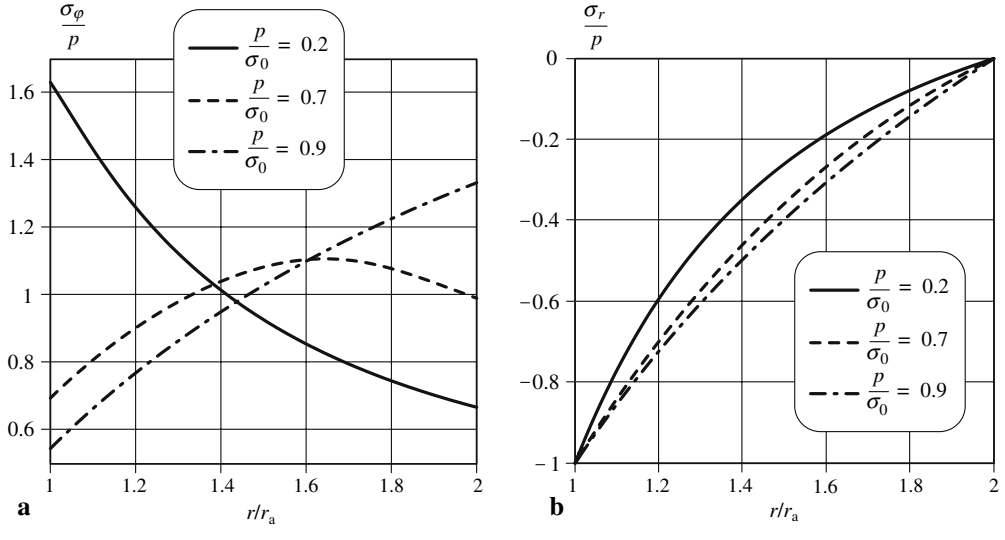

Fig. 6. Normalized stresses versus radial coordinate for $\zeta = 0.5$. **a** Hoop stress, **b** radial stress

CAX8R elements. Figure 7 illustrates the solutions based on the ABAQUS finite code and the approximate solutions of Eqs. (21)–(24). We observe that for different values of the normalized pressure the solutions are in a very good agreement.

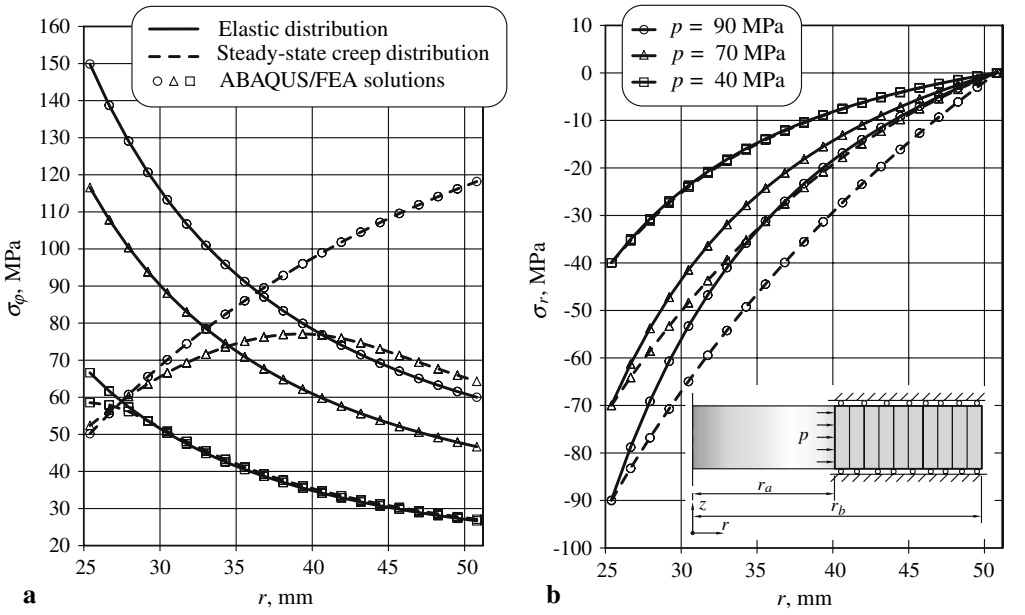

Fig. 7. Normalized stresses versus radial coordinate for $\zeta = 0.5$ using the presented method and ABAQUS finite element code. **a** Hoop stress, **b** radial stress

5 Conclusions

The aim of this paper was to describe the minimum creep rate for advanced heat resistant steels for both the linear and the power law creep ranges. The outcome is the Odqvist type creep constitutive equation with three material constants including the creep exponent n, the stress σ_0 characterizing the transition from the linear to the power law creep range as well as the reference creep rate $\dot{\varepsilon}_0$. The material constants are identified for 9Cr1MoVNb steel at 600 °C. To illustrate the influence of the linear creep on the structural behavior we presented an example for the pressurized thick cylinder. The results show that the character of the steady state stress distributions additionally depends on the normalized pressure $\tilde{p} = p/\sigma_0$. For low values of $\tilde{p}$ the cylinder behaves in the linear creep range. The hoop stress has the maximum on the inner surface. For high values of $\tilde{p}$ the classical power law type solution follows with the maximum hoop stress on the outer surface. For moderate values of $\tilde{p}$ both the linear and the power law creep ranges must be taken into account. The maximum of the hoop stress shifts towards the core of the cylinder. The range of validity of the classical solution depends on the material behavior and in particular, on the transition stress value σ_0. For materials with a narrow linear creep range, i.e. for small values of σ_0 the classical power law creep solution can be applied. For advanced heat resistant steels, however, σ_0 usually takes values between 50 and 100 MPa depending on the absolute temperature [4]. In this case the power law creep assumption may lead to misleading conclusions regarding the structural behavior under creep conditions.

Future studies should be related to the extension of the secondary creep model to account for temperature dependence as well as microstructure degradation processes like subgrain coarsening and creep cavitation. This can be accomplished by the introduction of appropriate Arrhenius type temperature functions and internal state variables.

References

[1] Betten, J.: Creep Mechanics. Springer, Berlin (2005)
[2] Naumenko, K., Altenbach, H.: Modelling of Creep for Structural Analysis. Springer, Berlin (2007)
[3] Frost, H.J., Ashby, M.F.: Deformation-Mechanism Maps. Pergamon, Oxford (1982)
[4] Kloc, L., Sklenička, V., Ventruba, J.: Comparison of low creep properties of ferritic and austenitic creep resistant steels. Mater. Sci. Engng. **A319–A321**, 774–778 (2001)
[5] Kloc, L., Sklenička, V.: Confirmation of low stress creep regime in 9% chromium steel by stress change creep experiments. Mater. Sci. Engng. **A387–A389**, 633–638 (2004)
[6] Odqvist, F.K.G.: Mathematical Theory of Creep and Creep Rupture. Oxford University Press, Oxford (1974)
[7] Skrzypek, J.J.: Plasticity and Creep. CRC Press, Boca Raton (1993)
[8] ABAQUS, Benchmarks Manual: ABAQUS, Inc. (2006)
[9] Leckie, F.A., Hayhurst, D.R.: Constitutive equations for creep rupture. Acta Metall. **25**, 1059–1070 (1977)
[10] Kostenko, Y., Lvov, G., Gorash, E., Altenbach, H., Naumenko, K.: Power plant component design using creep-damage analysis. In: Proceedings of IMECE2006, pp. 1–10. Chicago: ASME, IMECE2006-13710 (2006)
[11] Boyle, J.T., Spence, J.: Stress Analysis for Creep. Butterworth, London (1983)
[12] Hayhurst, D.R.: Creep rupture under multiaxial states of stress. J. Mech. Phys. Solids **20**, 381–390 (1972)
[13] Hyde, T.H., Sun, W., Becker, A.A.: Failure prediction for multi-material creep test specimens using steady-state creep rupture stress. Int. J. Mech. Sci. **42**, 401–423 (2000)
[14] Lee, J.S., Armaki, H.G., Maruyama, K., Muraki, T., Asahi, H.: Causes of breakdown of creep strength in 9Cr-1.8W-0.5Mo-VNb steel. Mater. Sci. Engng. **A428**, 270–275 (2006)
[15] Polcik, P., Sailer, T., Blum, W., Straub, S., Buršik, J., Orlová, A.: On the microstructural developmenr of the tempered martensitic Cr-steel P91 during long-term creep–a comparison of data. Mater. Sci. Engng. **A260**, 252–259 (1999)
[16] Penny, R.K., Mariott, D.L.: Design for Creep. Chapman & Hall, London (1995)
[17] Dyson, B.F., McLean, M.: Micromechanism-quantification for creep constitutive equations. In: Murakami, S., Ohno, N., (eds.) IUTAM Symposium on Creep in Structures, pp. 3–16. Kluwer, Dordrecht (2001)
[18] Kowalewski, Z.L., Hayhurst, D.R., Dyson, B.F.: Mechanisms-based creep constitutive equations for an aluminium alloy. J. Strain Anal. **29**(4), 309–316 (1994)
[19] Perrin, I.J., Hayhurst, D.R.: Creep constitutive equations for a 0.5Cr-0.5Mo-0.25V ferritic steel in the temperature range 600–675°C. J. Strain Anal. **31**(4), 299–314 (1994)
[20] Odqvist, F.K.G., Hult, J.: Kriechfestigkeit metallischer Werkstoffe. Springer, Berlin (1962)
[21] Backhaus, G.: Deformationsgesetze. Akademie-Verlag, Berlin (1983)
[22] Becker, A.A., Hyde, T.H., Sun, W., Andersson, P.: Benchmarks for finite element analysis of creep continuum damage mechanics. Comput. Mater. Sci. **25**, 34–41 (2002)